Environment International 126 (2019) 234–241

Contents lists available at ScienceDirect

Environment International

journal homepage: www.elsevier.com/locate/envint

# Formation of Cd precipitates on γ-$Al_2O_3$: Implications for Cd sequestration in the environment

Qian Sun[a,b], Cun Liu[a], Peixin Cui[a], Tingting Fan[c], Mengqiang Zhu[d], Marcelo Eduardo Alves[e], Matthew G. Siebecker[f,g], Donald L. Sparks[f], Tongliang Wu[a,b], Wei Li[h], Dongmei Zhou[a], Yujun Wang[a,*]

[a] Key Laboratory of Soil Environment and Pollution Remediation, Institute of Soil Science, The Chinese Academy of Sciences, Nanjing 210008, China
[b] University of Chinese Academy of Sciences, Beijing 100049, China
[c] Nanjing Institute of Environmental Sciences, Ministry of Environmental Protection of the People's Republic of China, Nanjing 210008, China
[d] Department of Ecosystem Science and Management, University of Wyoming, Laramie, Wyoming 82071, United States
[e] Departament of Exact Sciences 'Luiz de Queiroz' Agricultural College – ESALQ/USP, Piracicaba, SP 13418-900, Brazil
[f] Delaware Environmental Institute, Interdisciplinary Science and Engineering Laboratory, University of Delaware, Newark, DE, United States
[g] Department of Plant and Soil Science, Texas Tech University, Lubbock, TX 79409, United States
[h] Key Laboratory of Surficial Geochemistry, Ministry of Education, School of Earth Sciences and Engineering, Nanjing University, Nanjing 210008, China

ARTICLE INFO

Handling Editor: Yong-Guan Zhu

*Keywords:*
Cadmium
γ-$Al_2O_3$
Precipitation
Cd-Al layered double hydroxide
Cd hydroxide phases
$CdCO_3$

ABSTRACT

Apart from surface complexation, precipitation of minerals also plays an important role in reducing the mobility and transport of heavy metals in the environment. In this study, Cd(II) sorption species on surfaces of γ-$Al_2O_3$ at pH 7.5 were characterized using multiple techniques. Results show that in addition to adsorption complexes, Cd hydroxide phases ($Cd(OH)_2$ precipitates and $Cd_x(OH)_y$ polynuclear complexes) were formed at the initial stages of Cd(II) sorption and gradually transformed to $CdCO_3$ with time. In addition, Cd(II) formed Cd−Al layered double hydroxide (LDH) on γ-$Al_2O_3$ under various conditions, independent of temperature and Cd loadings. The formation of Cd hydroxide phases and Cd−Al LDH could be ascribed to surface-induced precipitation because the bulk solution was undersaturated with respect to hydroxides. Cd−Al LDH formation on the Al-bearing mineral here is rather surprising because typically this occurs with elements of ionic radii similar to that of $Al^{3+}$; this formation is unknown for metals such as Cd(II) with a much larger ionic radius. The thermodynamic feasibility of Cd−Al LDH formation was further confirmed by laboratory synthesis of Cd−Al LDH and density function theory (DFT) calculations. These results suggest that Cd precipitation on Al-bearing minerals can be an important mechanism for Cd immobilization in the natural environment. Additionally, the finding of Cd−Al LDH formation on Al-bearing minerals and the thermodynamic stability of Cd−Al LDH provides new insights into the remediation of Cd-polluted soils and aquatic systems.

## 1. Introduction

Mobility and transport of heavy metals in the environment is greatly affected by chemical processes such as sorption-desorption, oxidation-reduction, and precipitation-dissolution. Among them, the formation of carbonates and hydroxides strongly immobilize heavy metals. In alkaline pH, carbonates can act as a sink for metals such as Zn(II), Cd(II), Fe(II) and Mn(II) (Buekers et al., 2007; Pan et al., 2014). Multinuclear metal hydroxide complexes and precipitates can form upon heavy metal sorption onto metal oxides, soil clays and soils, even at metal loadings below a theoretical monolayer coverage, arising from the nucleation process at the solution-solid interface (Sparks, 2002). In comparison with single metal hydroxides, layered double hydroxides (LDHs) are more resistant to proton dissolution and thermodynamically more stable (Nachtegaal and Sparks, 2003; Siebecker et al., 2018). LDH has brucite-like metal-hydroxide layers with permanent positive charges arising from trivalent metal cations (e.g., $Al^{3+}$) in the layer. The positive charges are compensated by the formation of a layered structure where positive sheets are separated by a disordered layer of water molecules and counter anions such as $Cl^-$, $NO_3^-$, $CO_3^{2-}$ (Vichi and Alves, 1997; Yan et al., 2009). Formation of Me-Al LDHs is identified as a steady and important sink for some trace metals in the environment (Peltier et al., 2006). Me-Al LDHs can form upon sorption of $Zn^{2+}$, $Ni^{2+}$, or $Co^{2+}$ on the surfaces of Al-bearing minerals (Siebecker et al.,

* Corresponding author.
*E-mail address:* yjwang@issas.ac.cn (Y. Wang).

https://doi.org/10.1016/j.envint.2019.02.036
Received 8 January 2019; Received in revised form 14 February 2019; Accepted 14 February 2019

2018; Towle et al., 1997; Thompson et al., 1999; Ford and Sparks, 2000; Delacaillerie et al., 1995; Scheidegger et al., 1997) through the coprecipitation of metal ions with $Al^{3+}$ or the replacement of metal ions in the metal hydroxides by $Al^{3+}$ migrating from Al-bearing minerals (Siebecker et al., 2018; Yamaguchi et al., 2001). It has been shown that metal ions ($Zn^{2+}$, $Ni^{2+}$ and $Co^{2+}$), with ionic radii close to that of $Al^{3+}$ (0.54 Å), but not for those (e.g. $Pb^{2+}$) with much larger radii, can form Me-Al LDHs (Sparks, 2002).

Cadmium (Cd) is one of the most toxic metals in the environment and more mobile than other metals, which pose threats to human health (Tapia et al., 2010; Wu et al., 2012). Industrial and agricultural activities such as mining, smelting, fertilizers, and sewage sludge lead to serious Cd pollution in many areas of the world (Rehman et al., 2015). Al-bearing minerals are common minerals in the environment and could immobilize Cd(II) effectively (Vasconcelos et al., 2008; Gräfe et al., 2007; Papelis, 1995) Vasconcelos et al. (2008) reported that Cd (II) sorbed on kaolinite formed outer-sphere and inner-sphere surface complexes at pH 7 and 9, respectively. Gräfe et al. (2007) conducted Cd (II) sorption experiment on gibbsite and kaolinite, and reached the conclusion that Cd(II) sorption on kaolinite was mainly attributed to outer-sphere complexation while the bidentate-binuclear complex and hydrated dimer ($Cd_2(OH)_3{\cdot}4H_2O$) or small polynuclear $Cd_x(OH)_y$ complexes were the major species formed on gibbsite. According to Papelis (1995), Cd(II) was sorbed on Al oxides as mononuclear surface complexes. However, these investigations focused significantly on Cd(II) adsorption complexes, whereas surface precipitation could also be occurring. The radius of $Cd^{2+}$ (0.97 Å) is much larger than that of $Al^{3+}$, and it has not been shown to form LDH via surface sorption on Al-bearing minerals (Vasconcelos et al., 2008; Gräfe et al., 2007; Papelis, 1995).

In the present study, Cd(II) sorption experiments on γ-$Al_2O_3$ were conducted for 18 h and 70 d to examine whether Cd-rich minerals would be formed on γ-$Al_2O_3$ in addition to common Cd(II) adsorption complexes. γ-$Al_2O_3$ is widely used in environmental chemistry research as a model compound for the investigation of the immobilization mechanisms of heavy metals by Al-bearing minerals (Li et al., 2011). It is a model for natural Al-hydroxide phases (e.g., gibbsite) and Al oxide layers in 1:1 clay minerals (e.g., kaolinite) (Ren et al., 2015). The effect of temperature (25 °C–55 °C) on Cd(II) immobilization by γ-$Al_2O_3$ was also investigated because the uptake capacity and the sorbed species can be affected by temperature (Ren et al., 2013; Roth et al., 2012; Dong et al., 2012). Additionally, the thermodynamic feasibility of Cd—Al LDH formation was evaluated by laboratory synthesis of Cd—Al LDH and DFT calculations. This study provides insights into the surface precipitation mechanism for Cd(II) on Al-bearing minerals, which can contribute to Cd immobilization in the environment.

## 2. Materials and methods

All chemicals used here including $Cd(NO_3)_2$, $Al(NO_3)_3$, $CdCO_3$, $Cd(OH)_2$, $NaNO_3$ and 4-(2-hydroxyethyl)-1-piperazineethanesulfonic acid (HEPES) were of analytical grade or purer. γ-$Al_2O_3$ (99.99%) was purchased from Aladdin Chemistry Co. Ltd. (Shanghai, China). The mean particle size of γ-$Al_2O_3$ determined by TEM (JEM-2100F, JEOL, Japan) was ca. 30 nm (Fig. S1). The specific surface area of γ-$Al_2O_3$ obtained from BET measurement (3H-2000PM, Beishide, China) was 165.7 $m^2g^{-1}$. Ultrapure deionized water (> 18 MΩ·cm) was used for preparation of solutions and for rinsing.

### 2.1. Cd(II) sorption experiments on γ-$Al_2O_3$

Cd(II) sorption experiments on γ-$Al_2O_3$ were carried out under 25, 40 and 55 °C at pH 7.5 using 50 mM HEPES buffer and 50 mM $NaNO_3$ as the background electrolyte in 50-mL polypropylene centrifuge tubes. HEPES exhibits nearly no complexing properties and thus the interference of HEPES with Cd(II) sorption could be neglected (Nowack and Sigg, 1996; Good et al., 1966). Various aliquots of 50 mM $Cd(NO_3)_2$ were added to 40 mL of electrolyte solution (50 mM HEPES and 50 mM $NaNO_3$) to acquire a series of Cd(II) concentrations (0.022, 0.048, 0.097, 0.23, 0.48, 0.98, 1.4, 2.9, 5.6, 9.4, 12.2, 21.6 mM), followed by addition of 0.1 g γ-$Al_2O_3$. The upper concentration limit was selected to avoid the formation of $Cd(OH)_2$ precipitation in the bulk solution. The bulk solution is undersaturated with respect to $Cd(OH)_2$. After shaking for 18 h, 20 mL of suspension was taken out from each tube, centrifuged at 9000 rpm, filtered by 0.22-μm cellulose membrane filters and then the filtrate was analyzed for Al(III) concentration by an inductively coupled plasma-optical emission spectrometer (ICP-OES, iCAP7400, ThermoFisher, America), and for Cd(II) concentration by a flame atomic absorption spectrophotometer (AAS, Z-2000, Hitachi, Japan). Tubes containing the remaining 20 mL of reaction suspension were placed in water baths for prolonged aging at 25, 40 and 55 °C, respectively. After 70 d, the reaction suspensions were centrifuged and filtered prior to analysis of Al(III), Cd(II) and $NO_3^-$ concentrations. The solid phase acquired by centrifuging was rinsed with deionized water twice and freeze-dried for further analysis.

### 2.2. Characterization of cd-γ-$Al_2O_3$ sorption samples

The solid phases of Cd-γ-$Al_2O_3$ sorption samples were characterized by powder X-ray diffraction (XRD) (Ultima IV, Rigaku, Japan), transmission electron microscopy (TEM) and selected-area electron diffraction (SAED), and extended X-ray absorption fine structure (EXAFS) spectroscopy. The detailed characterization methods are given in the Supporting Information.

### 2.3. Synthesis and characterization of Cd—Al LDH

Cd—Al LDH was synthesized based on a previously published procedure (Vichi and Alves, 1997) as described in the Supporting Information. The synthesis conditions varied, including pH (7.5–10.0), temperature (25–55 °C), and reaction time (0–12 d). The synthesized Cd—Al LDHs were characterized by XRD. One representative LDH (synthesized at pH 8, 55 °C, aged for 22 h) was selected for the morphology and elementary composition analysis by scanning electron microscopy and energy dispersive spectroscopy (SEM-EDS, S—3400N II, HITACHI, Japan). The suspension was drop-cast onto copper tape and then coated with gold for the analyses.

### 2.4. DFT calculations of Mg—Al LDH substituted by $Zn^{2+}$, $Cd^{2+}$ or $Pb^{2+}$

DFT calculations were carried out for stepwise substitution of $Mg^{2+}$ by $Zn^{2+}$, $Cd^{2+}$ or $Pb^{2+}$ in bulk Mg—Al LDH ($Mg_2Al$-$CO_3$-LDH) to acquire the free energy of substitution. Details of DFT calculations were described in the Supporting Information.

## 3. Results and discussion

### 3.1. Sorption experiments

Cd(II) sorption experiments on γ-$Al_2O_3$ were carried out at 25, 40 and 55 °C at pH 7.5. Aqueous Cd(II) concentrations before and after γ-$Al_2O_3$ sorption for 18 h and 70 d at various temperatures are shown in Table S1. Corresponding Cd(II) sorption amounts are depicted in Fig. 1, which shows that the total amounts of Cd(II) sorbed for 70 d were much higher than those for 18 h. The increase in the sorption of Cd(II) with time was probably due to the high sorption affinity of γ-$Al_2O_3$ for Cd(II) which caused accumulation of Cd(II) on the mineral surface and the increase in Cd(II) precipitation on γ-$Al_2O_3$ surface over time.

### 3.2. Transmission electron microscopy

One sorption sample (0.23 mM Cd, 40 °C, 70 d) was selected as the

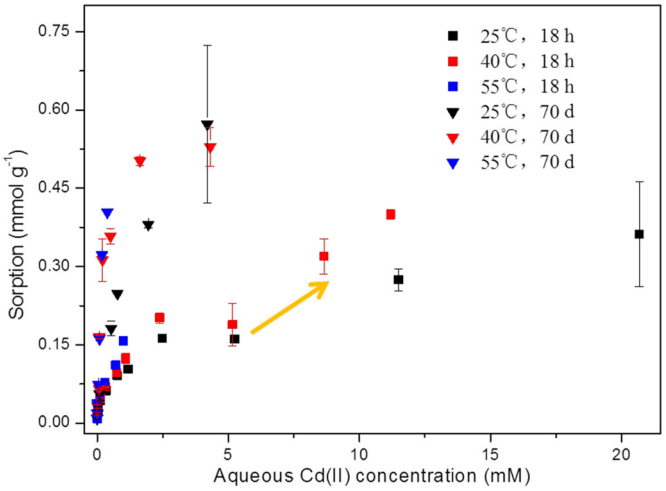


**Fig. 1.** Cd(II) sorption on γ-$Al_2O_3$ for 18 h and 70 d at 25, 40 and 55 °C. The yellow arrow indicates the sharp increase of the plot of the sorption amounts vs. aqueous Cd(II) concentrations for 18 h at initial Cd(II) concentration higher than 5.6 mM. (For interpretation of the references to colour in this figure legend, the reader is referred to the web version of this article.)

representative for the TEM analysis (Fig. 2). The flake-like material with morphology different from γ-$Al_2O_3$ was observed (Fig. 2a). The SAED pattern for the flake-like material shows multiple diffraction rings (Fig. 2b). The d-spacing is the inverse of the radius of the diffraction ring. The rings at 4.10, 2.84, 2.30, 1.96 and 1.39 Å correspond to (004), (110), (202), (116), and (222) reflection peaks of Cd−Al LDH respectively, verifying the formation of Cd−Al LDH in this sorption sample. This is the first experimental observation of Cd−Al LDH formation on Al-bearing materials. EXAFS and XRD analyses were further conducted to identify Cd−Al LDH and other possible Cd species in sorption samples.

### 3.3. EXAFS spectroscopy

$CdCO_3$, $Cd(OH)_2$, Cd−Al LDH, and Cd_pH 6 were chosen as reference standards for linear combination fitting (LCF) analysis of Cd(II) sorption samples with initial Cd(II) concentration at 0.23–5.6 mM (Fig. 3, Table 1). Cd_pH 6 represents adsorption complexes Cd formed on γ-$Al_2O_3$ (including both inner-sphere complexes and outer-sphere complexes) considering that no Cd precipitates ($CdCO_3$, $Cd(OH)_2$, Cd−Al LDH) could be generated at pH 6. $Cd(OH)_2$ represents Cd

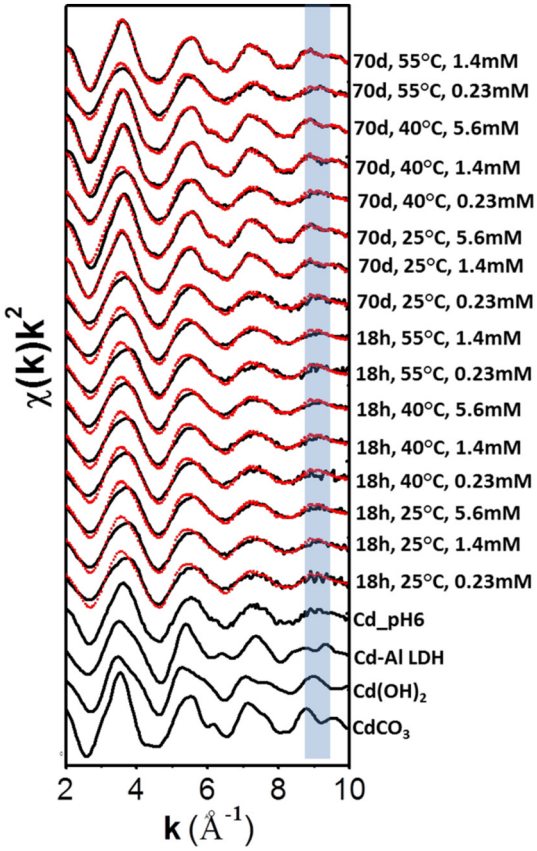


**Fig. 3.** LCF analysis of Cd K-edge EXAFS spectra for sorption samples. The blue shaded area is used to highlight the characteristic patterns of the reference compounds. The results of LCF analysis are listed in Table 1. (For interpretation of the references to colour in this figure legend, the reader is referred to the web version of this article.)

hydroxide phases ($Cd(OH)_2$ precipitates and $Cd_x(OH)_y$ polynuclear complexes). Based on LCF, Cd_pH 6 accounted for 38–80% of total sorbed Cd(II) in sorption samples, indicating that a large proportion of Cd(II) was adsorbed on γ-$Al_2O_3$ as surface complexes. $CdCO_3$ (23–43%) was present only in samples reacted for 70 d at initial Cd(II) concentrations of 1.39 mM and 5.63 mM. The $Cd(OH)_2$ fraction accounted for 31–51% in samples where no $CdCO_3$ was found and accounted for 0–14% in samples with $CdCO_3$ formed. Similarly, Cd hydroxide phases

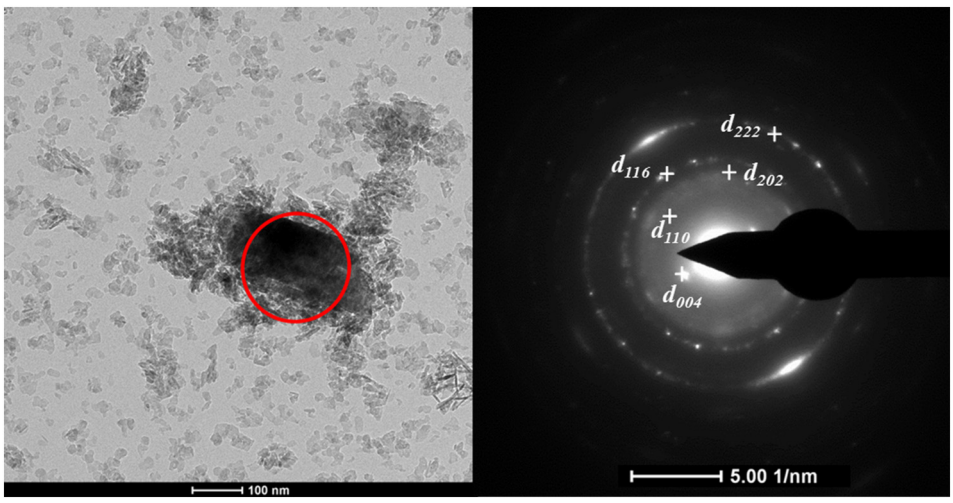


**Fig. 2.** (a) TEM images of selected Cd-loaded γ-$Al_2O_3$ (0.23 mM Cd, 40 °C, 70 d). (b) SAED pattern of the selected area in (a).

**Table 1**
Results of linear combination fits of $k^2$-weighted Cd K-edge EXAFS spectra. Fit range was 2–10 $Å^{-1}$.

| Experimental conditions | Components (%) | | | | | R-factor |
|---|---|---|---|---|---|---|
| | Cd_pH 6 | | $CdCO_3$ | $Cd(OH)_2$ | LDH | |
| Reacted for 18 h | | | | | | |
| 25 °C | 0.23 mM Cd(II) | 44 | 0 | 44 | 12 | 0.129 |
| | 1.4 mM Cd(II) | 44 | 0 | 48 | 8 | 0.101 |
| | 5.6 mM Cd(II) | 46 | 0 | 44 | 10 | 0.089 |
| 40 °C | 0.23 mM Cd(II) | 37 | 0 | 41 | 22 | 0.124 |
| | 1.4 mM Cd(II) | 44 | 0 | 42 | 15 | 0.100 |
| | 5.6 mM Cd(II) | 41 | 0 | 42 | 18 | 0.100 |
| 55 °C | 0.23 mM Cd(II) | 42 | 0 | 51 | 7 | 0.136 |
| | 1.4 mM Cd(II) | 38 | 0 | 45 | 17 | 0.109 |
| Reacted for 70 d | | | | | | |
| 25 °C | 0.23 mM Cd(II) | 51 | 0 | 38 | 11 | 0.083 |
| | 1.4 mM Cd(II) | 55 | 31 | 7 | 7 | 0.014 |
| | 5.6 mM Cd(II) | 80 | 23 | 1 | 0 | 0.032 |
| 40 °C | 0.23 mM Cd(II) | 58 | 0 | 31 | 11 | 0.042 |
| | 1.4 mM Cd(II) | 70 | 30 | 0 | 0 | 0.034 |
| | 5.6 mM Cd(II) | 43 | 43 | 14 | 0 | 0.019 |
| 55 °C | 0.23 mM Cd(II) | 41 | 0 | 31 | 28 | 0.072 |
| | 1.4 mM Cd(II) | 59 | 38 | 3 | 0 | 0.014 |

were reported to be formed on kaolinite (Gräfe et al., 2007), and red mud (Luo et al., 2011), as verified by EXAFS spectroscopy. The negative relationship between the amounts of Cd hydroxide phases and $CdCO_3$ could be interpreted by the gradual transformation of Cd hydroxide phases to $CdCO_3$ that has a higher thermodynamic stability.

Cd−Al LDH (7–28%) emerged in all samples except for those where the fraction of $CdCO_3$ was high. A beat pattern of the k-edge EXAFS spectrum for LDH appeared at 6.5 $Å^{-1}$ and 9.3 $Å^{-1}$, close to that for $CdCO_3$ (6.3 $Å^{-1}$, 9.5 $Å^{-1}$) (Fig. 3). The characteristic peaks of LDH might be masked by the contribution of $CdCO_3$, especially when the concentration of LDH was low, leading to no LDH fraction predicted by LCF results when the $CdCO_3$ fraction was high. The F-test was used to examine if the inclusion of LDH in these samples could significantly improve the goodness of fit. The highest confidence level (75.0%) was found in the sorption sample (0.23 mM Cd, 55 °C, 70 d) which had the highest proportion of LDH (28%), demonstrating that the LDH proportion would affect the confidence level. Unfortunately, the confidence level (α) was lower than the required 95% for the examined samples (Table S2), demonstrating that the inclusion of LDH in these samples could not significantly improve the goodness of fit, likely due to the relatively small percentage of LDH. Shell-by-shell fitting of Cd K-edge EXAFS spectra was further performed (Fig. S2, Table S3), which indicated that Cd−Al LDH and $CdCO_3$ were generated in sorption samples reacted for 70 d with initial Cd concentrations of 1.4 and 5.6 mM. In addition, shell fitting results confirmed the formation of inner-sphere complexes (i.e. chemisorption) in sorption samples. However, it is still difficult to know whether the outer-sphere complexes were also included in the 38–80% surface complexes based on the existing results. The detailed discussion on shell-by-shell fitting results are shown in the Supporting Information.

For Cd−Al LDH, the EXAFS spectrum has a distinctive beat pattern at 9.3 $Å^{-1}$ (Fig. 3). However, the EXAFS spectrum of $CdCO_3$ also has a beat pattern near this position, making it hard to detect the characteristic pattern of Cd−Al LDH when a large amount of $CdCO_3$ precipitates are formed. $Cd(OH)_2$ has a beat pattern at 8.8 $Å^{-1}$, which could also mask the splitting and dampening of the beat pattern at 8.8 $Å^{-1}$ of Cd−Al LDH. Thus, the distinctive beat pattern of Cd−Al LDH was nearly undetectable in our experiments because of the small amount of LDH and the coexistence of a relatively high amount of Cd hydroxide phases or $CdCO_3$.

Combining the LCF and shell-by-shell fitting results, the Cd phases formed on γ-$Al_2O_3$ are summarized as follows: In addition to the formation of adsorption complexes, LDH was formed under all conditions studied, regardless of temperature, reaction time and Cd loadings used in the present study. Cd hydroxide phases were formed within 18 h and then decreased sharply at initial Cd(II) concentrations of 1.4 and 5.6 mM for 70 d, which was presumably due to the transformation to $CdCO_3$.

### 3.4. X-ray diffraction

The characteristic peaks of $CdCO_3$ at 3.77 Å (23.6°), 2.94 Å (30.4°), 2.46 Å (36.4°), 2.07 Å (43.6°) and 1.84 Å (49.5°) were found in samples reacted for 18 h with initial Cd(II) concentration higher than 5.6 mM and for 70 d with initial Cd(II) concentration higher than 0.23 mM (Fig. 4a, b), consistent with EXAFS results. The sharp increase of the plot of the sorption amounts vs. aqueous Cd(II) concentrations for 18 h at initial Cd(II) concentration higher than 5.6 mM (Fig. 1) presumably resulted from the much higher amount of $CdCO_3$ formed than other precipitates under these conditions. At 70 d, the formation of $CdCO_3$ did not induce the sharp step of the plot of the sorption amounts vs. aqueous Cd(II) concentrations, which might be due to that a higher amount of adsorption complexes were formed than $CdCO_3$, as indicated by LCF analysis.

A subtle peak at 7.7 Å (11.5°) appeared for five of the sorption samples (Fig. 4c). Previous studies showed that the d-spacings in the layer stacking direction of synthetic Cd-Al-$CO_3$ LDH and Cd-Al-$NO_3$ LDH were 7.54 Å and 8.24 Å, respectively (Vichi and Alves, 1997). Considering that all other possible precipitate phases generated in the system ($CdCO_3$, $Al(OH)_3$, $Al_2O_3$, $Cd(OH)_2$) have no characteristic peak at this position and EXAFS results confirmed the formation of Cd−Al LDH in sorption samples, the peak at 7.7 Å could be ascribed to the mixture of Cd-Al-$CO_3$ LDH and Cd-Al-$NO_3$ LDH. Because the area determined using SAED was very small (about 100 nm) where only Cd-Al-$NO_3$ LDH was found while the bulk material was determined by XRD where Cd-Al-$CO_3$ LDH and Cd-Al-$NO_3$ LDH coexisted, the value of (002) reflection of LDH determined by SAED and XRD was slightly different. Cd-Al-$CO_3$ LDH and Cd-Al-$NO_3$ LDH exhibit similar polytypes, where anions locate at the interlayer space (Vichi and Alves, 1997; Yan et al., 2009). Although the concentration of $NO_3^-$ in the reaction solution was much higher than $CO_3^{2-}$, bivalent $CO_3^{2-}$ has a stronger anion exchange ability than monovalent $NO_3^-$ and the $CO_3^{2-}$-interlayered LDH is more thermodynamically stable than $NO_3^-$-interlayered LDH (Peltier et al., 2006), which would lead to the formation of the mixture of Cd-Al-$CO_3$ LDH and Cd-Al-$NO_3$ LDH. Four of the five sorption samples with the characteristic peak of LDH were reacted for 70 d, presumably because

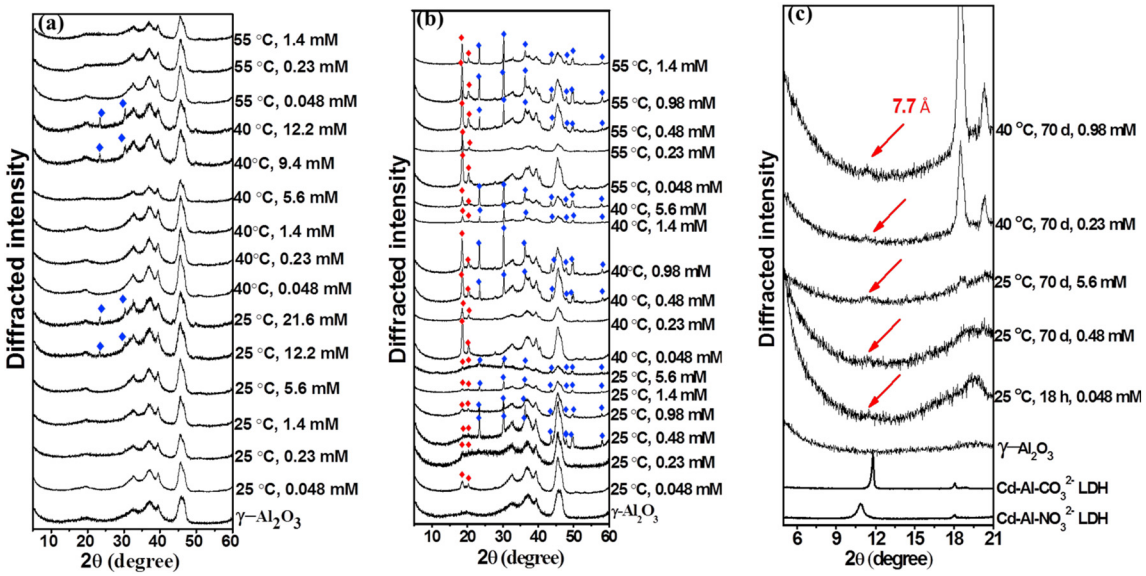


**Fig. 4.** XRD patterns of Cd-γ-$Al_2O_3$ sorption samples for 18 h (a) and 70 d (b). The blue and red diamonds denote the peaks of $CdCO_3$ and $Al(OH)_3$, respectively. (c) XRD patterns of selected samples are amplified at the range from 5° to 21° 2θ. Red arrows indicate the characteristic peaks of Cd—Al LDH. The XRD pattern of γ-$Al_2O_3$ is depicted at the bottom of the graphs for comparison. (For interpretation of the references to colour in this figure legend, the reader is referred to the web version of this article.)

the degree of crystallinity of LDH increased with the prolonged reaction time. The lack of LDH peaks visible by XRD in other sorption samples was likely due to the poor crystallinity of LDH. No obvious effects of temperature and Cd loadings on the formation of LDH were found under the conditions studied.

In addition to the precipitation of $CdCO_3$ and LDH in sorption samples, β-$Al(OH)_3$ (JCPDS No. 20-0011) was formed in sorption samples reacted for 70 d, indicated by the XRD peaks at 4.79 Å (18.5°) and 4.37 Å (20.3°) (Fig. 4b). Similarly, Lefèvre et al. (2002) reported that γ-$Al_2O_3$ was progressively transformed to β-$Al(OH)_3$. The formation of β-$Al(OH)_3$ can be attributed to the dissolution of γ-$Al_2O_3$ and reprecipitation as β-$Al(OH)_3$. It was reported that Al-bearing minerals have the following dissolution trend: γ-$Al_2O_3$ > corundum (α-$Al_2O_3$) > β-$Al(OH)_3$ > boehmite (γ-AlOOH) > gibbsite (α-$Al(OH)_3$) and Al dissolution was critical in the LDH formation (Siebecker et al., 2018; Li et al., 2012). The high Al dissolution capacity of γ-$Al_2O_3$ favored Cd—Al LDH formation in this study.

The characteristic peaks of γ-$Al_2O_3$ existed in every sorption samples. The radius of Cd(II) (0.97 Å) is much larger than Al(III) (0.54 Å). If Al(III) in γ-$Al_2O_3$ was substituted by Cd(II), the lattice cell of γ-$Al_2O_3$ would become larger. However, no left-shift of the XRD peaks of γ-$Al_2O_3$ was observed after Cd(II) sorption, indicating that substitution was unlikely responsible for Cd(II) immobilization. Comparing to the radius of Cd(II), the radii of Zn(II) (0.74 Å) and Ni(II) (0.69 Å) are more close to that of Al(III). The substitution of Al(III) by Zn(II) or Ni(II) has never been found in the abundant investigations on Zn(II) and Ni(II) sorption on Al-bearing minerals (Li et al., 2012; Yamaguchi et al., 2001; Nachtegaal and Sparks, 2003; Ren et al., 2015; Tan et al., 2014). Therefore, it is reasonable to speculate that Cd(II) was unable to replace Al(III) in the process of the sorption on γ-$Al_2O_3$.

The lack of the characteristic peaks of $Cd(OH)_2$ is likely due to the poor crystallinity of generated $Cd(OH)_2$ or the much higher amount of $Cd_x(OH)_y$ polynuclear complexes formation than $Cd(OH)_2$.

### 3.5. Thermodynamic analysis of the aqueous solutions in the sorption reactions and the driving forces for Cd(II) precipitation

Solution pH was measured after the reaction because pH was an important factor in precipitation. Solution pH was well buffered at ca. 7.5 at initial Cd(II) concentrations of 0.022–1.4 mM, but decreased to ca. 7.2 at initial Cd(II) concentrations of equal or higher than 2.9 mM. $CO_3^{2-}$ in the solution was derived from atmospheric $CO_2$. The saturation index of the aqueous solution with respect to $CdCO_3$ could be calculated assuming that aqueous $CO_3^{2-}$ was equilibrated with atmospheric $CO_2$. Although the saturation index for $CdCO_3$ was higher than 0 even at the lowest initial Cd(II) concentration (Table S6), $CdCO_3$ was only detected in sorption samples reacted for 18 h with initial Cd(II) concentration higher than 5.6 mM and for 70 d with initial Cd(II) concentration higher than 0.23 mM. The lack of $CdCO_3$ formation under other conditions was presumably due to the slow dissolution rate of $CO_2$ to the solution, the slow kinetics of $CdCO_3$ precipitation, and the removal of $CO_3^{2-}$ from solution as it incorporated into the LDH structure. XRD and EXAFS analyses demonstrated that a large amount of $CdCO_3$ was formed in some sorption samples, although the concentration of $CO_3^{2-}$ at pH 7.2–7.5 was very low (no more than $2.8 \times 10^{-7}$ M). This large amount of $CdCO_3$ was attributed to the gradual precipitation of $CO_3^{2-}$ with Cd(II) and its continuous supply by the atmospheric $CO_2$.

The solution pH was below the pH where the formation of $Cd(OH)_2$ would be expected to form via homogeneous precipitation according to the thermodynamic solubility product. Nevertheless, Cd hydroxide phases were detected by EXAFS analysis. Co(II), Ni(II), Cu(II) and Cr(III) have been reported to form metal hydroxide phases on phyllosilicates and oxides, in solutions undersaturated with respect to those hydroxides, which was referred to as surface-induced precipitation (Yamaguchi et al., 2001; O'Day et al., 1994; Scheidegger et al., 1996; O'Day, 1994; Charlet and Manceau, 1992; Xia et al., 1997) These metal hydroxide phases could form at metal loadings well below the monolayer coverage (Sparks, 2002). The reasons for the surface-induced precipitation where the solution is undersaturated with respect to the solid phase could be (Sparks, 2002): (1) the activity of the surface precipitate is < 1; (2) the dielectric constant of the solution near the solid surface is less than that of the solution, which lowers the solubility of the surface precipitate; (3) the solid surface could lower the nucleation energy by offering sterically similar sites. Cd hydroxide phases gradually transformed to $CdCO_3$ at high initial Cd(II) concentrations within 70 d, which could be explained by the gradual $CO_2$ concentrating in the solution and the higher thermodynamic stability of $CdCO_3$ than that of $Cd(OH)_2$.

The saturation index (25 °C) of the solution with respect to Cd-Al-

$CO_3$ LDH, of the formulation $Cd_2Al(OH)_60.5CO_3$, was estimated (Table S7). The calculation process is detailed in the Supporting Information. The saturation index at 25 °C was < 0 throughout Cd(II) concentration range examined, demonstrating that bulk solutions were undersaturated with respect to Cd-Al-$CO_3$ LDH at 25 °C. Considering the larger amount of Cd-Al-$CO_3$ LDH formed than Cd-Al-$NO_3$ LDH, as implied by XRD, it was reasonable to speculate that the bulk solutions were also undersaturated with respect to Cd-Al-$NO_3$ LDH. For samples reacted at 40 and 55 °C, a greater amount of LDH at higher temperatures was not detected by XRD and EXAFS. Thus, bulk solutions at 40 and 55 °C were unlikely saturated with respect to Cd-Al-$CO_3$ LDH. Based on these considerations, we propose that Cd—Al LDH in the sorption experiments was formed via the interfacial mechanisms, rather than homogeneous precipitation in the bulk solution. Similarly, Ni—Al LDH formation on pyrophyllite and gibbsite was reported to be generated in solution undersaturated with respect to Ni—Al LDH, which was attributed to surface-induced precipitation (Yamaguchi et al., 2001). Mechanisms of surface-induced precipitation have been discussed above. Two possible processes could describe Cd—Al LDH formation on γ-$Al_2O_3$ surface: (1) Cd(II) ions and Al(III) ions were concentrated on γ-$Al_2O_3$ surface via sorption and then precipitated as Cd—Al LDH; (2) Al (III) ions were released from γ-$Al_2O_3$ and replaced Cd(II) in Cd hydroxide phases, promoting the formation of Cd—Al LDH. Although dissolved Al(III) concentration in the solution was low (no more than $6 \times 10^{-7}$, detailed in the Supporting Information), the precipitation of Cd—Al LDH was surface-induced, which does not require ion activity product in the bulk solution to meet the solubility product. γ-$Al_2O_3$ acts as a source of dissolved Al(III) and continuously provides Al(III) for the formation of Cd—Al LDH. Compared to the adsorption to γ-$Al_2O_3$, the precipitation as LDH would be a more stable sink for Cd(II) because adsorbed Cd(II) could be desorbed by other cations, while Cd(II) in the crystal lattice of LDH is difficult to release. In addition, Cd—Al LDH precipitate in the natural environment could become more stable over time due to the diffusion of Si originating from the weathering into the interlayer space of the LDH, replacing the anions such as $CO_3^{2-}$ or $NO_3^-$ and forming a precursor Cd—Al phyllosilicate. Scheckel and Sparks (2001) reported that the replacement of Si for $NO_3^-$ in the interlayer of LDH led to an obviously increasing stability. Besides, the Ostwald ripening of the LDH precipitate could result in increased crystallization (Scheckel and Sparks, 2001), which was more stable.

In summary, Cd(II) immobilization mechanism on γ-$Al_2O_3$ could be described as follows: Firstly, Cd(II) was adsorbed to the surface of γ-$Al_2O_3$, forming adsorption complexes (38–80%). Meanwhile, Al(III) was gradually released from γ-$Al_2O_3$. Then, the local accumulation of Cd(II) and Al(III) on the mineral surface would result in the formation of Cd hydroxide phases (31–51%) and Cd—Al LDH (7–28%). The formation of Cd hydroxide phases and Cd—Al LDH could be ascribed to surface-induced precipitation because the bulk solution was undersaturated with respect to the two phases. In addition, Cd hydroxide phases would gradually transform to $CdCO_3$ (23–43%) with time when initial Cd(II) concentration was high, which could be explained by the gradual $CO_2$ concentrating in the solution and the higher thermodynamic stability of $CdCO_3$ than that of Cd hydroxide phases.

The similarity and difference of Cd(II) immobilization mechanisms between γ-$Al_2O_3$ and other types of Al-bearing minerals could be acquired by comparing Cd(II) sorption mechanism on γ-$Al_2O_3$ in the present study with those on other Al-bearing minerals reported by previous investigators (Vasconcelos et al., 2008; Gräfe et al., 2007; Papelis, 1995). Vasconcelos et al. (2008) reported that Cd(II) sorbed on kaolinite for 4 h formed outer-sphere and inner-sphere surface complexes at pH 7 and 9, respectively. Gräfe et al. (2007) conducted Cd(II) sorption experiment on gibbsite and kaolinite for 12 h, and reached the conclusion that Cd(II) sorption on kaolinite was mainly attributed to outer-sphere complexation while the bidentate-binuclear complex and hydrated dimer ($Cd_2(OH)_3{\cdot}4H_2O$) or small polynuclear $Cd_x(OH)_y$ complexes were the major species formed on gibbsite. According to Papelis (1995), Cd(II) was sorbed on Al oxides after 24 h as mononuclear surface complexes. In our studies, Cd(II) adsorption complexes and Cd hydroxide phases were also found to form on γ-$Al_2O_3$, similar to the results reported by previous studies. Thus, we could conclude that the formation of Cd(II) adsorption complexes and Cd hydroxide phases are the common Cd(II) immobilization mechanisms by Al-bearing minerals, independent of the type of adsorbents. The formation of adsorption complexes could be ascribed to the sufficient sorption sites on Al-bearing minerals while the formation of Cd hydroxide phases could be explained by the local accumulation of adsorbed Cd(II) on the mineral surface. Notably, in our studies, when the initial Cd(II) concentration was high, the formed Cd hydroxide phases would gradually transform to $CdCO_3$ with time. Besides, Cd(II) formed Cd—Al layered double hydroxide (LDH) on γ-$Al_2O_3$ under various conditions, independent of temperature and Cd loadings. In contrast, the formation of $CdCO_3$ and Cd—Al LDH was not observed in previous studies (Vasconcelos et al., 2008; Gräfe et al., 2007; Papelis, 1995). The lack of $CdCO_3$ formation in previous studies could be attributed to that $CO_2$ was not sufficiently concentrated in the solution in the short period of time (no more than 24 h) and the applied Cd(II) concentration was low (no more than 1 mM). $CdCO_3$ formation is expected to be favorable when dissolved Cd (II) concentration is high or the reaction time is long enough. Generally, LDH formation was considered to be most limited by the rate of Al dissolution of minerals (Sparks, 2002) because LDHs were thermodynamically unstable if Al substitution was < 20% (Tan et al., 2014). For example, the formation of Zn—Al LDH and Ni—Al LDH has been shown to be highly related to mineral surface dissolution (Li et al., 2012; Yamaguchi et al., 2001). The formation of LDHs was found to be more favorable on Al-bearing minerals with higher Al dissolution. Thus, in previous studies, the inability of Cd—Al LDH formation could be attributed to the limited Al dissolution amount of the sorbents such as gibbsite and kaolinite in the short reaction time (no more than 24 h). In contrast, γ-$Al_2O_3$ has a high Al dissolution capacity, which would favor Cd—Al LDH formation even within a short time. It was reasonable to speculate that if the reaction time is long enough, sufficient Al(III) would release from Al-bearing minerals such as gibbsite and kaolinite, and then produce Cd—Al LDH.

### 3.6. The evaluation of the influence of environmental factors on Cd(II) immobilization by Al-bearing minerals

In the natural environment, the environmental factors (e.g., pH condition, Cd level, competitive cations, organic matter) would greatly affect Cd immobilization on Al-bearing minerals. Based on the experimental results in this study, despite the low Cd concentration, Cd(II) could still form adsorption complexes, Cd hydroxide phases, and Cd—Al LDH in the process of Cd(II) sorption to Al-bearing minerals. However, Cd(II) would precipitate as $CdCO_3$ at the low Cd concentration only if the period of time is long enough. The immobilization mechanism would vary with reaction pH. Both precipitation (formation of $CdCO_3$, Cd hydroxide phases, Cd—Al LDH) and adsorption would contribute to Cd(II) immobilization by Al-bearing minerals under natural and alkaline conditions while only adsorption complexation would account for Cd(II) immobilization under acidic pH. In addition, other metal cations (e.g. $Pb^{2+}$, $Zn^{2+}$, $Ni^{2+}$) would compete with Cd(II) for the adsorption sites on Al-bearing minerals, and thus inhibiting Cd(II) adsorption. Considering that both Cd hydroxide phases and Cd—Al LDH are formed via surface-induced precipitation, where the adsorption process is the premise, the formation of Cd hydroxide phases and Cd—Al LDH would also be suppressed due to the competition of metal cations. Similarly, the formation of $CdCO_3$ would be hindered because of the precipitation of $CO_3^{2-}$ by other metal cations. Moreover, the presence of organic matter would interfere with Cd(II) immobilization on Al-bearing minerals. Organic matter could play a complex role in Cd(II) adsorption on Al-bearing minerals. Organic matter might increase Cd(II) adsorption via the formation of ternary complexes on the mineral surface or

decrease Cd(II) adsorption via the complexation of Cd(II) to dissolved organic matter (Benyahya and Garnier, 1999). The effect of organic matter on Cd(II) adsorption is dependent on pH, the type and concentration of organic matter and the type of adsorbent. Yamaguchi et al. (2001) and Nachtegaal and Sparks (2003) reported that humic acid, citrate, and salicylate would suppress the formation of Zn−Al LDH in the immobilization of Zn by Al-bearing minerals, which could be interpreted by the complexation of Zn(II) and Al(III) and the blockage of the surface sites. We could therefore speculate that the existence of the organic matter would also slow the formation of Cd−Al LDH. Meanwhile, organic matter is expected to inhibit the formation of Cd hydroxide phases and $CdCO_3$ precipitates via the complexation with Cd (II).

### 3.7. XRD and SEM-EDS analyses of the synthesized Cd−Al LDHs

Considering that Cd−Al LDH formation on Al-bearing minerals is a novel mechanism for Cd(II) sequestration, the stability of Cd−Al LDH from a thermodynamic perspective was further examined. Cd−Al LDHs were synthesized under various conditions, including varying pH (7.5–10.0), temperature (25–55 °C) and reaction time (0–12 d). The characteristic peaks of Cd−Al LDH (JCPDS Card: NO. 43-0478) appeared in the XRD patterns of the synthesized products under all conditions (Fig. S4). A few investigations have reported the syntheses of Cd−Al LDHs, which were carried out under alkaline pH (pH 8–10) and high temperature (70–90 °C) (Vichi and Alves, 1997; Pérez et al., 2007; Hansen et al., 2009) The formation of Cd−Al LDHs at mild pH (pH 7.5) and ambient temperature (25 °C) within a short period of time in our study suggested that the formation of Cd−Al LDH is thermodynamically feasible under environmentally relevant conditions.

The interlayer d-spacing of LDH (Vichi and Alves, 1997) i.e., the peak position of 003 reflection (~8.20 Å), varied with pH and temperature. With pH increasing from 8 to 10, the interlayer spacing shifted from 8.20 to 8.00 Å (Fig. S4a). The interlayer spacings of LDHs synthesized at 25, 40 and 55 °C were 8.08, 8.18 and 8.30 Å, respectively (Fig. S4b). The observed smaller interlayer spacings of LDHs at higher pH and lower temperature might be due to the larger proportion of Cd-Al-$CO_3$ LDH at higher pH and lower temperature resulting from the higher concentration of $CO_3^{2-}$ introduced in the solution. The degree of crystallinity for the sample aged for 12 d was significantly higher than that without aging (Fig. S4c), consistent with XRD results for sorption samples that four of the five sorption samples with the characteristic peak of LDH were reacted for 70 d.

One of the synthesized Cd−Al LDHs (synthesized at pH 8, 55 °C, aged for 22 h) was selected as a representative LDH to examine the morphology by SEM. Well-crystallized lamellar structure was observed and the particle size ranged from 0.2 μm to 2 μm (Fig. S5a, b). EDS was applied to examine the relative amounts of Cd and Al in the selected areas. The calculated molar ratios of Cd/Al were 1.9:1 for area III and 2.0:1 for area IV, respectively (Fig. S5c, d), nearly equal to the 2:1 ratio of Cd/Al in LDH (i.e., Al substitution in LDH at 0.33), indicating that in those locations most added Cd(II) and $Al^{3+}$ contributed to the formation of LDH instead of the formation of single metal hydroxides such as $Cd(OH)_2$ and $Al(OH)_3$. Thus, it could be inferred that LDH was the dominant species in the precipitates, suggesting the thermodynamic stability of Cd−Al LDH over $Cd(OH)_2$ and $Al(OH)_3$ phases.

### 3.8. DFT calculations of Mg−Al LDH substituted by $Zn^{2+}$, $Cd^{2+}$ or $Pb^{2+}$

Apart from the laboratory experiments, DFT calculations of Mg−Al LDH substituted by $Zn^{2+}$, $Cd^{2+}$ or $Pb^{2+}$ were used to evaluate the thermodynamic stability of LDH. The substitution of $Mg^{2+}$ by $Zn^{2+}$, $Cd^{2+}$ or $Pb^{2+}$ causes a lattice relaxation due to the difference in ionic radii. These plausible geometries were then characterized by first-principle DFT calculations, from which the relative thermodynamic stability of bulk Zn−Al LDH, Cd−Al LDH and Pb−Al LDH compared to Mg−Al LDH was assessed.

After structural relaxation, the metal-O bond length increased slightly to 2.11 Å and 2.26 Å for Zn−Al LDH and Cd−Al LDH, respectively, but rather significantly to 2.53 Å for Pb−Al LDH, compared with the corresponding Mg−O bond of 2.10 Å. Good agreement was found between our periodic-structure-based DFT calculations of metal-O bond lengths and the cluster DFT calculations as well as the experimental values (Yan et al., 2009). While the cluster DFT calculated metal-O bond lengths are slightly longer than the experimental ones due to neglecting the interaction of the small cluster with neighboring atoms in the lattice (2.191, 2.301 and 2.463 Å for Mg−O, Zn−O and Cd−O, respectively), the periodic DFT calculations predicted slightly shorter bond lengths compared to the experimental values but within the systematic uncertainty of DFT methods. The substitution of larger cations such as Pb and Cd caused lattice expansion with the lattice parameter increased to a = b = 11.32 Å, c = 8.03 Å, and a = b = 11.64 Å, c = 8.26 Å, respectively. The lattice expansion gives rise to an increase in the bond strength and would influence on the relative stability of different phases. Consequently, the estimated average energy of substitution of $Zn^{2+}$, $Cd^{2+}$ and $Pb^{2+}$ for $Mg^{2+}$ in Mg−Al LDH per cation site was −2.787, 0.098, 3.955 eV, respectively (Fig. 5), suggesting that it was thermodynamically favorable for $Zn^{2+}$ but unfavorable for $Pb^{2+}$ to substitute for $Mg^{2+}$ in Mg−Al LDH. Interestingly, Cd−Al LDH has a similar energetic stability to Mg−Al LDH although it was less stable than Zn−Al LDH in accordance with the binding energy trends calculated by the cluster DFT method (Yan et al., 2009). Considering that the structure of Mg−Al LDH is very stable, the substitution energy for $Mg^{2+}$ indicating that Zn−Al LDH is easy to form agrees well with the experimental findings that in addition to Mg−Al LDH, Zn−Al LDH was one of the most commonly natural LDHs in soils (Tan et al., 2014; Trainor et al., 2000; Aucour et al., 2015). Our calculation also predicts that Cd−Al LDH is relatively stable, in agreement with our experimental findings. Furthermore, it could be inferred that Pb−Al LDH is unlikely to form, which has been previously reported (Sparks, 2002). This thermodynamic assessment via isolated DFT clusters in a reductionist system is necessary to get a better understanding of Cd−Al LDH stability. Given the large cationic radius of Cd, the inclusion of the DFT results provide convincing data for the Cd−Al LDH stability. Importantly, the stability of Cd−Al LDH formation via theoretical calculations was consistent with the empirical experimental results of the Cd−Al LDH formation on γ-$Al_2O_3$, implying the potential formation of Cd−Al LDH in the environment.

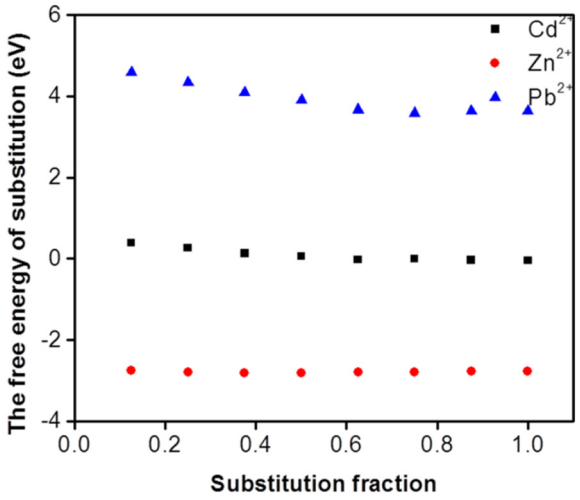


**Fig. 5.** The free energy of substitution for $Mg^{2+}$ in Mg−Al LDH by $Cd^{2+}$, $Zn^{2+}$ and $Pb^{2+}$ respectively. $Mg^{2+}$ in the supercell was gradually substituted by $Cd^{2+}$, $Zn^{2+}$ and $Pb^{2+}$ until $Mg^{2+}$ was completely displaced.

## 4. Conclusions

Our results show that at pH 7.5, in addition to common adsorption complexes, surface-induced Cd hydroxide phases were formed on γ-$Al_2O_3$ within a short period of time and gradually transformed to $CdCO_3$. The long reaction time or high Cd(II) concentration is essential for $CdCO_3$ formation. Noteworthy, Cd−Al LDH was formed on γ-$Al_2O_3$ via surface-induced precipitation, which has not been reported previously. Cd−Al LDH formation was thermodynamically feasible under environmentally relevant conditions, evidenced by laboratory syntheses and DFT calculations, consistent with the formation of Cd−Al LDH on γ-$Al_2O_3$.

In comparison to adsorption complexes, the formation of precipitates is a much more stable sink for heavy metals immobilized by minerals in the environment and deserves attention. Although the Cd content in soils is relatively low, our study shows that Cd precipitates could form on the Al oxide over a wide concentration range of Cd(II). Thus, it is necessary to consider Cd precipitates in the modeling and prediction of Cd speciation as well as risk assessments for the migration and transformation of Cd in the environment. In addition, the finding of Cd−Al LDH formation on Al-bearing minerals and the thermodynamic stability of Cd−Al LDH provides new insights into the remediation of Cd at contaminated sites, since LDH is less prone to proton dissolution than the pure metal hydroxides (Nachtegaal and Sparks, 2003). Further studies are required to explore effects of other environmental factors such as pH and organic matter on the formation of Cd precipitates.

## Acknowledgements

This study was supported by the National Key Research and Development Program of China (2018YFC1800503), Natural Science Foundation of Jiangsu Province, China (BE2018760), the National Natural Science Foundation of China (projects No. 41771276), and the 135 Frontier Projects of Institute of Soil Science, Chinese Academy of Sciences (ISSASIP1619). We are also grateful to the Shanghai Synchrotron Radiation Facility (SSRF) for use of the synchrotron radiation facilities at beamline 14W.

## Appendix A. Supplementary data

This document contains information regarding characterization of Cd-γ-$Al_2O_3$ sorption samples, the synthesis of Cd−Al LDH, DFT calculations, results of the shell-by-shell fitting of EXAFS spectra for sorption samples, the calculation of the saturation index of Cd−Al LDH, Figs. S1–S5, and Tables S1–S7. Supplementary data to this article can be found online at https://doi.org/10.1016/j.envint.2019.02.036.

## References

Aucour, A.M., Bedell, J.P., Queyron, M., Magnin, V., Testemale, D., Sarret, G., 2015. Dynamics of Zn in an urban wetland soil-plant system: coupling isotopic and EXAFS approaches. Geochim. Cosmochim. Acta 160, 55–69.
Benyahya, L., Garnier, J.M., 1999. Effect of salicylic acid upon trace-metal sorption (Cd, Zn, Co, and Mn) onto alumina, silica, and kaolinite as a function of pH. Environ. Sci. Technol. 33 (33), 1398–1407.
Buekers, J., Van, L.L., Amery, F., Van, B.S., Maes, A., Smolders, E., 2007. Role of soil constituents in fixation of soluble Zn, Cu, Ni and Cd added to soils. Eur. J. Soil Sci. 58 (6), 1514–1524.
Charlet, L., Manceau, A.A., 1992. X-ray absorption spectroscopic study of the sorption of Cr(III) at the oxide-water interface: II. Adsorption, coprecipitation, and surface precipitation on hydrous ferric oxide. J. Colloid Interface Sci. 148 (2), 443–458.
Delacaillerie, J.B.D., Kermarec, M., Clause, O., 1995. Impregnation of gamma-alumina with Ni(II) or Co(II) ions at neutral pH: hydrotalcite-type coprecipitate formation and characterization. J. Am. Chem. Soc. 117 (46), 11471–11481.
Dong, Y., Liu, Z., Li, Y., Chen, L., Zhang, Z., 2012. Effect of pH, ionic strength, foreign ions, fulvic acid and temperature on $^{109}$Cd(II) sorption to γ-$Al_2O_3$. J. Radioanal. Nucl. Chem. 292 (2), 619–627.
Ford, D.G., Sparks, D.L., 2000. The nature of Zn precipitates formed in the presence of pyrophyllite. Environ. Sci. Technol. 34 (12), 2479–2483.
Good, N.E., Winget, G.D., Winter, W., Connolly, T.N., Izawa, S., Singh, R.M.M., 1966. Hydrogen ion buffers for biological research. Biochemistry 5 (2), 467–477.
Gräfe, M., Singh, B., Balasubramanian, M., 2007. Surface speciation of Cd(II) and Pb(II) on kaolinite by XAFS spectroscopy. J. Colloid Interface Sci. 315 (1), 21–32.
Hansen, B., Curtius, H., Odoj, R., 2009. Synthesis of a Mg-Cd-Al layered double hydroxide and sorption of selenium. Clay Miner. 57 (3), 330–337.
Lefèvre, G., Duc, M., Lepeut, P., Caplain, R.A., Fédoroff, M., 2002. Hydration of γ-alumina in water and its effects on surface reactivity. Langmuir 18 (20), 7530–7537.
Li, W., Harrington, R., Tang, Y., Kubicki, J.D., Aryanpour, M., Parise, J., Phillips, B., 2011. Differential pair distribution function study of the structure of arsenate adsorbed on nanocrystalline γ-alumina. Environ. Sci. Technol. 45 (22), 9687–9692.
Li, W., Xu, W., Livi, K.J.T., Siebecker, M.G., Wang, Y., Phillips, B.L., Sparks, D.L., 2012. Formation of crystalline Zn-Al layered double hydroxide precipitates on γ-alumina: the role of mineral dissolution. Environ. Sci. Technol. 46 (21), 11670–11677.
Luo, L., Ma, C., Ma, Y., Zhang, S., Lv, J., Cui, M., 2011. New insights into the sorption mechanism of cadmium on red mud. Environ. Pollut. 159 (5), 1108–1113.
Nachtegaal, M., Sparks, D.L., 2003. Nickel sequestration in a kaolinite-humic acid complex. Environ. Sci. Technol. 37 (3), 529–534.
Nowack, B., Sigg, L., 1996. Adsorption of EDTA and metal-EDTA complexes onto goethite. J. Colloid Interface Sci. 177 (1), 106–121.
O'Day, P.A., 1994. Molecular structure and binding sites of cobalt(II) surface complexes on kaolinite from X-ray absorption spectroscopy. Clay Clay Miner. 42 (3), 337–355.
O'Day, P., Jr, G., Parks, G., 1994. X-ray absorption spectroscopy of cobalt(II) multinuclear surface complexes and surface precipitates on kaolinite. J. Colloid Interface Sci. 165 (2), 269–289.
Pan, Y., Koopmans, G.F., Bonten, L.T.C., Song, J., Luo, Y., Temminghoff, E.J.M., Comans, R.N.J., 2014. Influence of pH on the redox chemistry of metal (hydr)oxides and organic matter in paddy soils. J. Soils Sediments 14 (10), 1713–1726.
Papelis, C., 1995. X-ray photoelectron spectroscopic studies of cadmium and selenite adsorption on aluminum oxides. Environ. Sci. Technol. 29 (6), 1526–1533.
Peltier, E., Allada, R., Navrotsky, A., Sparks, D.L., 2006. Nickel solubility and precipitation in soils: a thermodynamic study. Clay Clay Miner. 54 (2), 153–164.
Pérez, M.R., Barriga, C., Fernández, J.M., Rives, V., Ulibarri, M.A., 2007. Synthesis of Cd/(Al + Fe) layered double hydroxides and characterization of the calcination products. J. Solid State Chem. 180 (12), 3434–3442.
Rehman, M.Z., Rizwan, M., Ghafoor, A., Naeem, A., Ali, S., Sabir, M., Qayyum, M.F., 2015. Effect of inorganic amendments for in situ stabilization of cadmium in contaminated soils and its phyto-availability to wheat and rice under rotation. Environ. Sci. Pollut. R. 22 (21), 1–10.
Ren, X., Yang, S., Hu, F., He, B., Xu, J., Tan, X., Wang, X., 2013. Microscopic level investigation of Ni(II) sorption on Na-rectorite by EXAFS technique combined with statistical F -tests. J. Hazard. Mater. 2-10, s252–s253.
Ren, X., Tan, X., Hayat, T., Alsaedi, A., Wang, X., 2015. Co-sequestration of Zn(II) and phosphate by γ-$Al_2O_3$: from macroscopic to microscopic investigation. J. Hazard. Mater. 297, 134–145.
Roth, E., Mancier, V., Fabre, B., 2012. Adsorption of cadmium on different granulometric soil fractions: influence of organic matter and temperature. Geoderma s189–190, 133–143.
Scheckel, K.G., Sparks, D.L., 2001. Dissolution kinetics of nickel surface precipitates on clay mineral and oxide surfaces. Soil Sci. Soc. Am. J. 65 (3), 685–694.
Scheidegger, A.M., Lamble, G.M., Sparks, D.L., 1996. Investigation of Ni sorption on pyrophyllite: an XAFS study. Environ. Sci. Technol. 30 (2), 548–554.
Scheidegger, A.M., Lamble, G.M., Sparks, D.L., 1997. Spectroscopic evidence for the formation of mixed-cation hydroxide phases upon metal sorption on clays and aluminum oxides. J. Colloid Interface Sci. 186 (1), 118–128.
Siebecker, M.G., Li, W., Sparks, D.L., 2018. The important role of layered double hydroxides in soil chemical processes and remediation: what we have learned over the past 20 years. Adv. Agron. 147, 1–59.
Sparks, D.L., 2002. Environmental soil chemistry. Soil Sci. 162 (3), 229–231.
Tan, X., Fang, M., Ren, X., Mei, H., Shao, D., Wang, X., 2014. Effect of silicate on the formation and stability of Ni-Al LDH at the γ-$Al_2O_3$ surface. Environ. Sci. Technol. 48 (22), 13138–13145.
Tapia, Y., Cala, V., Eymara, E., Frutos, I., Gárate, A., Masaguer, A., 2010. Chemical characterization and evaluation of composts as organic amendments for immobilizing cadmium. Bioresour. Technol. 101 (14), 5437–5443.
Thompson, H.A., Parks, G.A., Brown, G.E., 1999. Dynamic interactions of dissolution, surface adsorption, and precipitation in an aging cobalt(II)-clay-water system. Geochim. Cosmochim. Acta 63 (11 − 12), 1767–1779.
Towle, S.N., Bargar, J.R., Brown, G.E., Parks, G.A., 1997. Surface precipitation of Co(II)(aq) on $Al_2O_3$. J. Colloid Interface Sci. 187 (1), 62–82.
Trainor, T.P., Brown, G.E., Parks, G.A., 2000. Adsorption and precipitation of aqueous Zn (II) on alumina powders. J. Colloid Interface Sci. 231 (2), 359–372.
Vasconcelos, I.F., Haack, E.A., Maurice, P.A., Bunker, B.A., 2008. EXAFS analysis of cadmium(II) adsorption to kaolinite. Chem. Geol. 249 (3–4), 237–249.
Vichi, F.M., Alves, O.L., 1997. Preparation of Cd/Al layered double hydroxides and their intercalation reactions with phosphonic acids. J. Mater. Chem. 7 (8), 1631–1634.
Wu, X., Jia, Y., Zhu, H., 2012. Bioaccumulation of cadmium bound to ferric hydroxide and particulate organic matter by the bivalve M. meretrix. Environ. Pollut. 165 (165), 133–139.
Xia, K., Bleam, W.F., Mehadi, A., Taylor, R.W., 1997. X-ray absorption and electron paramagnetic resonance studies of Cu(II) sorbed to silica: surface-induced precipitation at low surface coverages. J. Colloid Interface Sci. 185 (1), 252–257.
Yamaguchi, N.U., Scheinost, A.C., Sparks, D.L., 2001. Surface-induced nickel hydroxide precipitation in the presence of citrate and salicylate. Soil Sci. Soc. Am. J. 65 (3), 729–736.
Yan, H., Wei, M., Ma, J., Li, F., Evans, D.G., Duan, X., 2009. Theoretical study on the structural properties and relative stability of M(II) − Al layered double hydroxides based on a cluster model. J. Phys. Chem. A 113 (21), 6133–6141.